Original Article

LncRNA *HEIH* modulates the proliferation, migration, and invasion of hepatocellular carcinoma cells by regulating the *miR-193a-5p/CDK8* axis

Yening Huang, Dongming Li, Lu Lu, Dan Song, Peng Li^

Department of Hepatobiliary and Pancreatic Surgery, The Second Affiliated Hospital of Hainan Medical University, Haikou, China

Contributions: (I) Conception and design: P Li; (II) Administrative support: P Li; (III) Provision of study materials or patients: P Li; (IV) Collection and assembly of data: P Li; (V) Data analysis and interpretation: P Li; (VI) Manuscript writing: All authors; (VII) Final approval of manuscript: All authors.

Correspondence to: Peng Li, MD. Department of Hepatobiliary and Pancreatic Surgery, The Second Affiliated Hospital of Hainan Medical University, No. 48 Baishuitang Road, Haikou 570100, China. Email: lipeng@hainmc.edu.cn.

Background: Hepatocellular carcinoma (HCC), a malignant tumor with a high mortality rate, is a serious problem worldwide. This research sought to examine how long non-coding RNA (lncRNA) high expression in hepatocellular carcinoma (*HEIH*) affects the development and progression of HCC.

Methods: The expression of *HEIH* in HCC patients and HCC cell lines was measured by quantitative real-time polymerase chain reaction (qRT-PCR). Additionally, HEIH was knocked down, and 3-(4,5-dimethylthiazol-2-yl)-2,5-diphenyl-2H-tetrazolium bromide, wound-healing and transwell assays were conducted to evaluate the effects of *HEIH* on the proliferation, migration, and invasion of the HCC cells, respectively. A xenografted mice model was constructed to investigate the function of *HEIH* on HCC tumorigenesis *in vivo*. The interactions among *HEIH*, microRNA (miR)-193a-5p and cyclin-dependent kinase 8 (*CDK8*) were also investigated by dual luciferase reporter (DLR) gene and RNA immunoprecipitation (RIP) assays.

Results: *HEIH* was highly expressed in HCC tissues, and was correlated with advanced TNM stage and the absence of vascular invasion. The *in vitro* experiments showed that silencing *HEIH* restrained the viability, migration, and invasion of HCC cells, and hampered xenograft tumor growth *in vivo*. Additionally, *HEIH* was shown to bind directly to microRNA 193a-5p (*miR-193a-5p*) and facilitate the expression of the target gene *CDK8* in the HCC cells. *CDK8* overexpression and *miR-193a-5p* silencing attenuated the effects of si-*HEIH*-induced inhibition on the proliferation, migration, and invasion of HCC cells.

Conclusions: Silencing *HEIH* restrained the proliferation, migration, and invasion of HCC cells via the *miR-193a-5p/CDK8* axis.

Keywords: Hepatocellular carcinoma (HCC); long non-coding RNA high expression in hepatocellular carcinoma (lncRNA *HEIH*); microRNA 193a-5p (*miR-193a-5p*); cyclin-dependent kinase 8 (*CDK8*)

Submitted Dec 05, 2023. Accepted for publication Jan 24, 2024. Published online Jan 29, 2024.
doi: 10.21037/tcr-23-2228
View this article at: https://dx.doi.org/10.21037/tcr-23-2228

^ ORCID: 0009-0001-0750-2770.

Introduction

Primary hepatocellular carcinoma (HCC) is a prevailing malignant tumor, and represents a major health-care challenge in the population (1). Previous research suggests that primary HCC is associated with genetic factors, alcoholism, obesity, viral infections, and metabolic diseases (2,3). Currently, surgical treatment is the main treatment strategy for primary HCC. However, most primary HCC is diagnosed at advanced stages, and many patients with HCC miss the opportunity for surgical treatment (4). Currently, there are no efficient methods for treating advanced HCC (5,6). Thus, further research determining the pathogenesis of HCC and identifying the causative factors in the progression of HCC is of critical significance for the development of therapeutic drugs for HCC.

Long non-coding RNA (lncRNA) is discovered as mRNA-like transcripts that do not encode proteins, ranging in length from 200 nt to 100 kb (7). There is increasing evidence that lncRNAs exert pivotal functions in the pathological processes of tumorigenesis (8,9). Multiple lncRNAs have been shown to be involved in the progression and development of HCC. For example, lncRNA-taurine upregulated 1 (*TUG1*) promotes the growth and metastasis of HCC (10). LncRNA CEBPA divergent transcript (*CEBPA-DT*) contributes to HCC metastasis via discoidin domain receptor tyrosine kinase 2 (DDR2)/beta-catenin activation (11). Further, lncRNA high expression in hepatocellular carcinoma (*HEIH*) has been shown to play a pro-tumor role in diverse cancer types (12,13). For example, *HEIH* accelerates the malignant development of gastric cancer by regulating glycolysis and autophagy (14). A high expression of *HEIH* is associated with a poor prognosis in non-small cell lung cancer, and contributes to the diagnosis of the disease (15). Zhao *et al.* demonstrated that *HEIH* inhibition impedes cell viability, migration and invasion, and enhances cell apoptosis in breast cancer (16). In addition, a recent study has shown that silencing *HEIH* suppresses HCC cell growth and metastasis (17). However, the specific action and the regulatory mechanism of *HEIH* in HCC have not been fully elucidated.

MicroRNA (miRNA or miR) is a non-coding RNA with a length of 20–24 nt that can regulate the stability and translation efficiency of target messenger RNA (mRNA) (18). MiRNA mediates a variety of biologic processes, such as cell growth, apoptosis, metabolic signal transduction and differentiation (19). Extensive research has been conducted on the abnormal expression of miRNA in normal and tumor tissues, and this research has emphasized the correlation between miRNA expression and cancer development (20). For example, *miR-29a* controls hypoxia inducible factor 1 subunit alpha (HIF-1α)/angiopoietin (ANGPT) signaling thereby inhibiting the incidence of HCC (21). *MiR-1-494p* has also been shown to downregulate basic helix-loop-helix ARNT like 1 (*BMAL1*) to promote lipid biosynthesis, resulting in the growth and metastasis of HCC (22). *MiR-3180* inhibits lipid synthesis and uptake to suppress HCC progression (23). *MiR-193a-5p* has been shown to play an anti-tumor (ovarian cancer) or pro-tumor role (renal cell carcinoma, pancreatic cancer) in several malignant tumors, including HCC (24-28). *MiR-193a-5p* has been identified as a novel biomarker in the recurrence and prognosis of HCC (27). It has been reported that *miR-193a-5p* overexpression hampers cell viability and invasion in HCC (28). Additionally, *miR-193a-5p* is highly expressed in HCC tissues, and accelerates the proliferation of and inhibits the apoptosis of HCC cells (29). These studies show the important function of *miR-193a-5p* in HCC. However, the regulatory relationship and between *HEIH* and *miR-193a-5p* remains unverified.

In this study, a sequence of *in vitro* and *in vivo* studies were performed to examine the potential action mechanisms of *HEIH*, *miR-193a-5p*, and cyclin-dependent kinase 8 (*CDK8*) in HCC. It also sought to examine the underlying mechanism of HCC and identify a novel therapeutic target for HCC treatment. We present this article in accordance

Highlight box

Key findings

- Silencing long non-coding RNA (lncRNA) high expression in hepatocellular carcinoma (*HEIH*) restrained the proliferation, migration, and invasion of hepatocellular carcinoma (HCC) cells via the microRNA 193a-5p (*miR-193a-5p*)/cyclin-dependent kinase 8 (*CDK8*) axis.

What is known, and what is new?

- Silencing lncRNA *HEIH* inhibits the growth and metastasis of HCC cells. *MiR-193a-5p* overexpression hinders the progression of HCC.
- LncRNA *HEIH* binds to *miR-193a-5p* to promote *CDK8* expression in HCC cells. Silencing *HEIH* inhibits HCC progression via the *miR-193a-5p/CDK8* axis.

What is the implication, and what should change now?

- This study provides a useful perspective for interventions in HCC progression. LncRNA *HEIH* could be used as a potential therapeutic target in HCC therapy in the future.

with the MDAR and ARRIVE reporting checklists (available at https://tcr.amegroups.com/article/view/10.21037/tcr-23-2228/rc).

Methods

Specimens

In total, 59 pairs of HCC tissues and adjacent normal tissues were acquired from HCC patients at the Second Affiliated Hospital of Hainan Medical University. None of the patients underwent chemotherapy or radiotherapy before the surgery. All the samples were stored in liquid nitrogen awaiting research. The current investigation was approved by the Ethics Committee of the Second Affiliated Hospital of Hainan Medical University (No. LW20210018). Informed consent was obtained from all the patients. This study was conducted in accordance with the Declaration of Helsinki (as revised in 2013).

Cell culture and transfection

Normal human HCC cell lines (huh7, hep3B, smmc-7721, and sk-Hep-1) and human hepatocytes (L02) were obtained from the Cell Ba 133-138nk of Type Culture Collection (CBTCC, Shanghai, China). The experimental cells were incubated in Dulbecco's Modified Eagle Medium (DMEM; Gibco, Grand Island, NY, USA) with 10% fetal bovine serum (FBS; Gibco) at 37 ℃, 5% CO_2 in a humidified incubator.

Short interfering RNA against *HEIH* (si-*HEIH*-1 and si-*HEIH*-2), the negative control (si-NC), the pcDNA3.1 vector targeting *HEIH*, and the empty vector were obtained from the RiboBio Company (Beijing, China). The *miR-193a-5p* mimics/inhibitor was designed by GenePharma (Shanghai, China). Hep3B and sk-Hep-1 were transfected with these plasmids using Lipofectamine 3000 (Invitrogen, Carlsbad, CA, USA). At 48 hours post-transfection, quantitative real-time polymerase chain reaction (qRT-PCR) was used to determine the efficiency of the transfection.

qRT-PCR

The total RNA was extracted from the prepared cells, and the HCC and adjacent tissues using TRIzol (Invitrogen). A Revert Aid First Strand Complementary DNA Synthesis Kit (Thermo Fisher Scientific, Waltham, MA, USA) was used to reverse transcribe the RNA into cDNA. MRNA expression was detected using SYBR Green PCR Master Mix (Takara, Dalian, China) on an ABI-Prism 7300 System (Applied Biosystem Foster City, CA, USA). The reaction conditions were as follows: 95 ℃ for 5 minutes, followed by 40 cycles of 94 ℃ for 30 s, and 60 ℃ for 30 s. The primer sequences were as follows: glyceraldehyde-3-phosphate dehydrogenase (*GAPDH*), forward 5'-CATCTTCTTTTGCGTCGCCA-3', reverse 5'-TTAAAAGCAGCCCTGGTGACC-3'; *HEIH*, forward 5'-CCTCTTGTGCCCCTTTCTT-3', reverse 5'-ATGGCTTCTCGCATCCTAT-3'; *miR-193a-5p*, forward 5'-GATAGCCTGATGTTATCA-3', reverse 5'-GTCTGGTGAGTTGGCG-3'; *CDK8*, forward 5'-GCCGGTTGTCAAATCCCTTAC-3', reverse 5'-TGTGACTGCTGTCTTGATTCCCT-3'; *U6*, forward 5'-CAAATTCGTGAAGCGTTCCATA-3', reverse 5'-AGTGCAGGGTCCGAGGTATTC-3'. All the data were analyzed using the $2^{-\Delta\Delta Ct}$ method with GAPDH as the endogenous control.

3-(4,5-dimethylthiazol-2-yl)-2,5-diphenyl-2H-tetrazolium bromide (MTT) assays

A total of 1×10^6 transfected Hep3B and sk-Hep-1 cells were inoculated in 96-well plates for 24, 48, 72, and 96 hours. MTT (Solarbio, Beijing, China) was appended to the wells of 96-well plates and hatched for four hours at 37 ℃. After incubation, the samples were dissolved in dimethyl sulfoxide (Solarbio). The absorbance was estimated at 450 nm by a microplate reader (Thermo Fisher Scientific).

Wound healing assays

The transfected Hep3B and sk-Hep-1 cells (1×10^6) were seeded in 6-well plates and incubated overnight. After the cells reached 80–90% confluence, a horizontal line was drawn using a 10-μL pipette tip. After being incubated with serum-free medium for eight hours, the width closure was captured by a microscope (Olympus, Tokyo, Japan) at the time points of 0 and 24 hours.

Transwell assays

The transfected Hep3B and sk-Hep-1 cells were incubated in the upper chambers with Matrigel (BD Biosciences, Franklin Lakes, NJ, USA). Next, DMEM medium (with 10% FBS) was added to the lower chambers. After 24 hours, the invasive cells in the lower chambers were fixed with

4% paraformaldehyde, and the cells in the upper chambers were cleared out. Next, the cells in the lower chambers were dyed with crystal violet dye and rinsed with phosphate buffered saline. The images were obtained by a microscope (Olympus), and the numbers of invasive cells were counted in f random fields.

Dual luciferase reporter (DLR) gene assays

The potential binding sites of *HEIH* and *miR-193a-5p* were predicted using starBase 3.0 (https://rnasysu.com/encori/), and the possible target region between binding sites and *miR-193a-5p* was predicted by the TargetScan (https://www.targetscan.org/vert_80/). The wide-type (WT) fragment of *HEIH* containing the *miR-193a-5p* binding sites or mutant (mut) sequences were cloned into pmirGLO dual luciferase vectors (Promega, Madison, WI, USA) to generate pmirGLO-WT-*HEIH* or pmirGLO-Mut-*HEIH*. Next, the Hep3B and sk-Hep-1 cells were co-transfected with pmirGLO-WT-*HEIH*/pmirGLO-Mut-*HEIH* and *miR-193a-5p* mimics/NC using Lipofectamine 3000 (Invitrogen). The luciferase activity was assessed using the Dual Luciferase Reporter System (Promega).

RNA immunoprecipitation (RIP) assays

The RIP assays were conducted using the imprint RIP kit (Sigma-Aldrich, St. Louis, MO, USA). In brief, the Hep3B and sk-Hep-1 cells were lysed by RIP lysis buffer (Solarbio). Next, the lysates were hatched with Argonaute2 antibody (Ago2, ab32381, Abcam, Cambridge, MA, USA) or immunoglobulin G (IgG) antibody (negative control, ab150077, Abcam). Then, protein A magnetic beads were added to isolate the immunoprecipitation complex. RNA was transcribed using an AmpliScribe T7-Flash Biotin-RNA Transcription Kit (Epicenter, Sausalit, CA, USA). Finally, the relative enrichment of *HEIH* and *miR-193a-5p* was examined by qRT-PCR.

Western blot assays

The proteins were obtained by RIPA buffer (Thermo Fisher Scientific). Next, the obtained proteins were isolated via sodium dodecyl-sulfate polyacrylamide gel electrophoresis and transferred onto a polyvinylidene fluoride membrane. Subsequently, the membrane was hatched with appropriate primary antibodies, CDK8, ab224828 (Abcam), and β-actin (ab8227, Abcam). Next, the membrane was hatched with the corresponding secondary antibody (ab150077, Abcam). The protein blots were developed using an enhanced chemiluminescence kit (Amersham, Little Chalfont, UK).

Animal study

BALB/c nu/nu mice (6 weeks old, 18–20 g) were obtained from SPF Biotechnology Co., Ltd (Beijing, China). The experimental mice were divided into the following three groups (n=8): Blank, si-NC, and si-HEIH-1 groups. The mice in the si-NC group and si-HEIH group received a retro-orbital intravenous (i.v.) injection of si-NC or si-*HEIH* transfected Hep3B cells (1×10^6), respectively. The mice in the blank group received no treatment. Tumor volume was measured every seven days as and calculated as follows: tumor volume = (length × width^2)/2. Four weeks later, all the mice were anesthetized by isoflurane inhalation and executed by cervical dislocation. The tumors were carefully excised for weighing. A protocol was prepared before the study without registration. All animal experiments were approved by the Ethics Committee of the Second Affiliated Hospital of Hainan Medical University (No. LW20210018), in compliance with national guidelines for the care and use of animals.

Statistical analysis

All the data are presented as the mean ± standard deviation and were analyzed using SPSS 22.0 statistical software (SPSS Inc., Chicago, IL, USA). Comparisons between two groups were analyzed by the *t*-test. Comparisons among multiple groups were analyzed by a one-way analysis of variance followed by Tukey's test. A P value <0.05 was considered statistically significant.

Results

HEIH expression was upregulated in HCC tissues

As *Figure 1A* shows, *HEIH* expression was significantly more increased in the HCC tissues than the adjacent tissues (P<0.001). The clinicopathological features of the HCC patients are set out in *Table 1*. A high expression of *HEIH* was significantly correlated with advanced TNM stage and an absence of vascular invasion. Additionally, the qRT-PCR results showed that *HEIH* expression was significantly more elevated in TNM stage III/IV than TNM stage I/II (P<0.01, *Figure 1B*). Consistent with the data in the clinical samples,

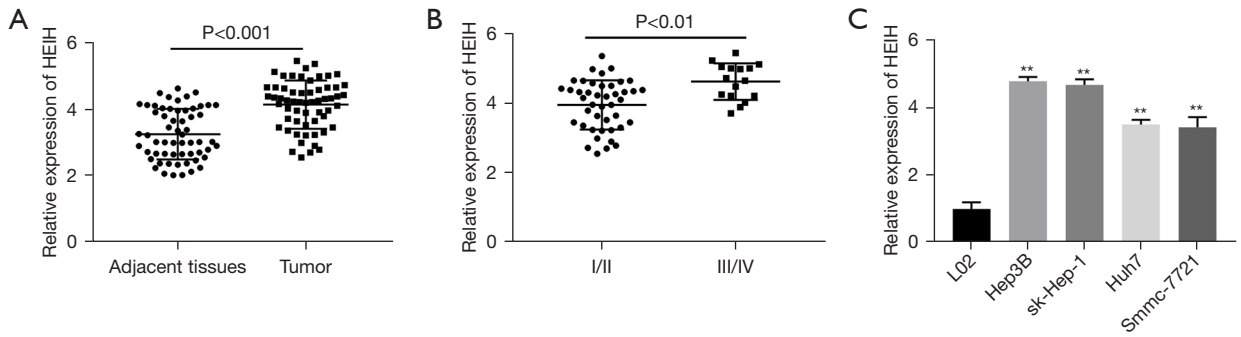

Figure 1 *HEIH* was upregulated in HCC tissues and cell lines. (A) *HEIH* expression in HCC tissues (N=59) and adjacent normal tissues (N=59) was detected by qRT-PCR. (B) Comparison of *HEIH* expression in TNM stage I/II and III/IV. (C) *HEIH* expression in HCC cell lines. **, P<0.01 *vs.* L02. HEIH, high expression in hepatocellular carcinoma; HCC, hepatocellular carcinoma; qRT-PCR, quantitative real-time polymerase chain reaction.

Table 1 Correlation between *HEIH* expression levels and the clinicopathological features of HCC patients

Variable	Total	*HEIH* expression		P value
		Low (N=24)	High (N=35)	
Age				0.372
<50 years	23	11	12	
≥50 years	36	13	23	
Gender				0.109
Male	39	13	26	
Female	20	11	9	
Tumor size				0.291
<5 cm	32	15	17	
≥5 cm	27	9	18	
AFP				0.341
<400 ng/mL	29	10	19	
≥400 ng/mL	30	14	16	
TNM stage				0.036*
I/II	43	21	22	
III/IV	16	3	13	
Vascular invasion				0.004**
Present	42	22	20	
Absent	17	2	15	

*, P<0.05; **, P<0.01. HEIH, high expression in hepatocellular carcinoma; HCC, hepatocellular carcinoma; AFP, alpha-fetoprotein; TNM, tumor-node-metastasis.

HEIH expression was significantly more increased in the HCC cell lines (Hep3B, sk-Hep-1, Huh7, and Smmc-7721) than the normal liver cell line (L02) (P<0.01, *Figure 1C*). Due to their relatively higher *HEIH* expression, the Hep3B and sk-Hep-1 cells were used in the subsequent experiments.

Silencing HEIH suppressed the viability, migration, and invasion of HCC cells in vitro, and hampered HCC tumorigenesis in vivo

To detect the function of *HEIH* in HCC, *HEIH* was inhibited by transfecting si-HEIH into the Hep3B and sk-Hep-1 cells. As expected, the qRT-PCR results indicated that *HEIH* expression was significantly reduced by si-*HEIH*-1 and si-*HEIH*-2 in both the Hep3B and sk-Hep-1 cells (P<0.01, *Figure 2A*). As it had lower *HEIH* expression, si-*HEIH*-1 was chosen for the subsequent experiments. The cell viability, wound-healing rate, and number of invasion cells were all significantly reduced by *HEIH* silencing in the Hep3B cells, and similar outcomes were observed in the sk-Hep-1 cells (P<0.01, *Figure 2B-2D*). To further validate the functional role of *HEIH in vivo*, xenograft models were built by inoculating Hep3B cells stably transfected with si-NC or si-*HEIH* into nude mice, and tumor growth was examined after 4 weeks. As *Figure 2E,2F* show, the tumor volume and tumor weight were significantly more decreased in the si-HEIH-1 group than the si-NC group (P<0.05). Taken together, all the above results showed that silencing *HEIH* impeded the viability, migration, and invasion of HCC cells *in vitro*, and suppressed xenograft tumor growth *in vivo*.

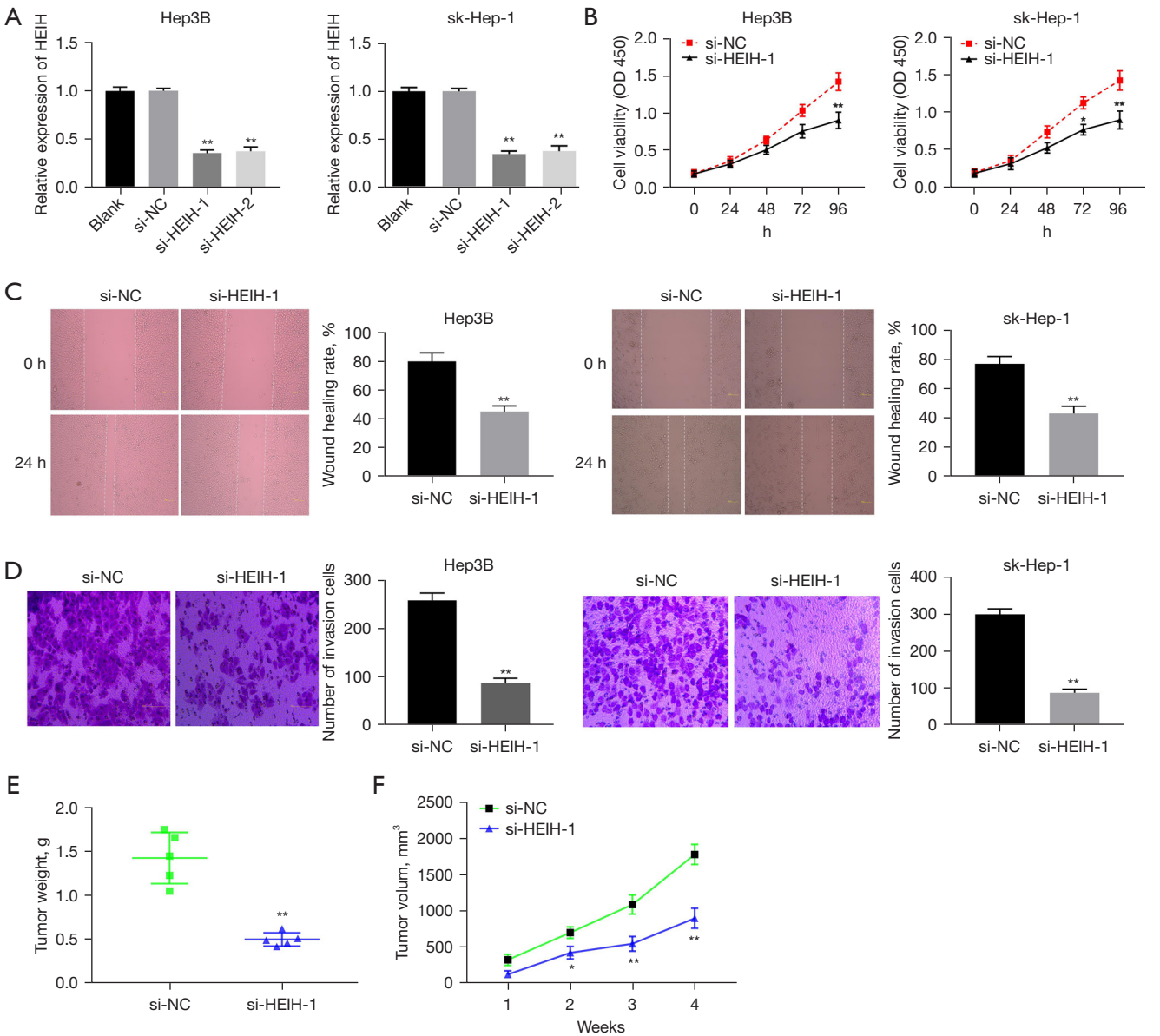

Figure 2 Silencing *HEIH* suppressed the proliferation, migration, and invasion of HCC cells. (A) The transfection efficiency of Hep3B and sk-Hep-1 cells was assessed by qRT-PCR; (B) cell viability was measured by MTT assays; (C) a wound-healing analysis was conducted to measure the migration of Hep3B and sk-Hep-1 cells (scar bar =100 μm, ×200); (D) the invasion of Hep3B and sk-Hep-1 cells was detected by transwell assays (crystal violet staining, scar bar =100 μm, ×400); (E) the tumor weights of the mice were quantified at 4 weeks post-injection; (F) the growth curves of the xenograft tumors were drawn by the tumor volume at 4 weeks post-injection. *, P<0.05 and **, P<0.01 *vs.* Blank (A) or si-NC (B-F). HEIH, high expression in hepatocellular carcinoma; HCC, hepatocellular carcinoma; qRT-PCR, quantitative real-time polymerase chain reaction; MTT, 3-(4,5-dimethylthiazol-2-yl)-2,5-diphenyl-2H-tetrazolium bromide.

MiR-193a-5p was a target gene of HEIH

The interaction between *HEIH* and *miR-193a-5p* in HCC was examined. First, starBase was used to predict the putative binding sites of *miR-193a-5p* in *HEIH* (*Figure 3A*). Si-*HEIH*-1 significantly induced the increase of the *miR-193a-5p* levels in both cells (P<0.01, *Figure 3B*). Additionally, the binding was further confirmed by dual luciferase reporter (DLR) assays. The results showed that

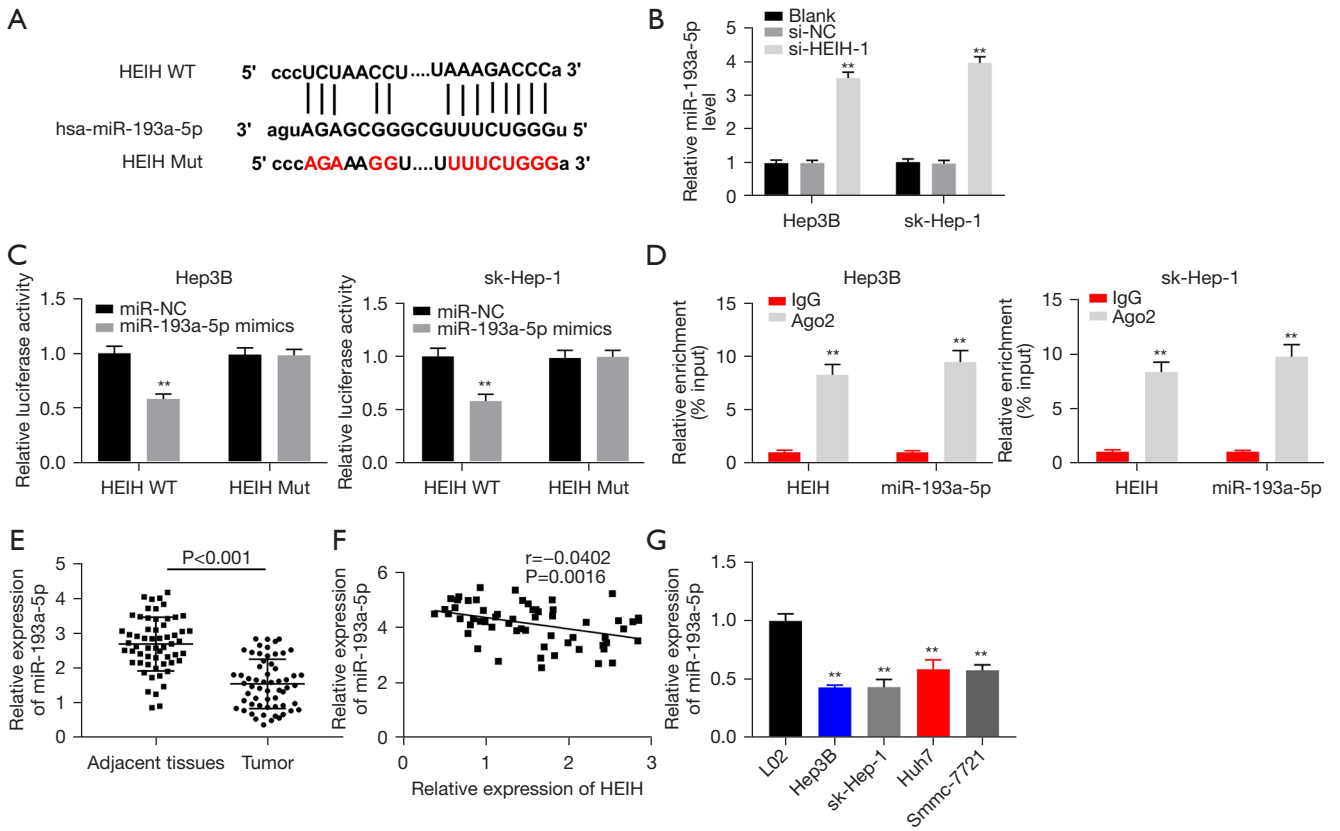

Figure 3 *MiR-193a-5p* was a target gene of *HEIH*. (A) Starbase online was used to predict the binding sites of *miR-193a-5p* and *HEIH*; (B) silencing *HEIH*-1 escalated the expression level of *miR-193a-5p*; (C) the relationship between *HEIH* and *miR-193a-5p* was verified by DLR gene assays; (D) the combination of *HEIH* and *miR-193a-5p* RNA was confirmed by binding protein immunoprecipitation (RIP) assays; (E) the expression of *miR-193a-5p* in the tumor tissues and adjacent tissues; (F) the correlation between *miR-193a-5p* expression and *HEIH* was analyzed by a Spearman's analysis; (G) *miR-193a-5p* expression in the HCC cell lines. **, P<0.01 *vs.* Blank (B), miR-NC (C), IgG (D), or L02 (G). HEIH, high expression in hepatocellular carcinoma; WT, wild-type; miR-193a-5p, microRNA 193a-5p; IgG, immunoglobulin G; DLR, dual luciferase reporter; RIP, RNA immunoprecipitation.

the relative luciferase activity was significantly decreased in the Hep3B and sk-Hep-1 cells co-transfected with *miR-193a-5p* mimics and *HEIH*-WT; however, no significant change was observed in the Hep3B and sk-Hep-1 cells co-transfected with miR-NC and *HEIH*-WT or *HEIH*-Mut (P<0.01, *Figure 3C*). The RIP assays indicated that *HEIH* and *miR-193a-5p* were both enriched in the precipitation of the Ago2 antibody but not in the precipitation of the IgG antibody, which suggests that they coexist in the RNA-induced silencing complex in the Hep3B and sk-Hep-1 cells (P<0.01, *Figure 3D*). Further, *miR-193a-5p* was significantly under expressed in the HCC tissues (P<0.001, *Figure 3E*). Subsequently, the correlation between *HEIH* and *miR-193a-5p* was examined by a Spearman's analysis. An inverse correlation was detected between the expression of *HEIH* and *miR-193a-5p* (r=−0.0402, P=0.0016, *Figure 3F*). *MiR-193a-5p* expression was reduced in the HCC cell lines, especially in the Hep-3B and sk-Hep-1 cells (P<0.01, *Figure 3G*).

MiR-193a-5p overexpression restrained cell viability, migration, and invasion in HCC

To examine the involvement of *miR-193a-5p* in the functional actions of *HEIH* in HCC, *miR-193a-5p* was overexpressed via the transfection of *miR-193a-5p* mimics and inhibited via the transfection of a *miR-193a-5p* inhibitor. As expected, the level of *miR-193a-5p* was significantly increased in the miR-193a-5p mimics group, and significantly decreased in the miR-193a-5p inhibitor group (P<0.01, *Figure 4A*). The cell viability,

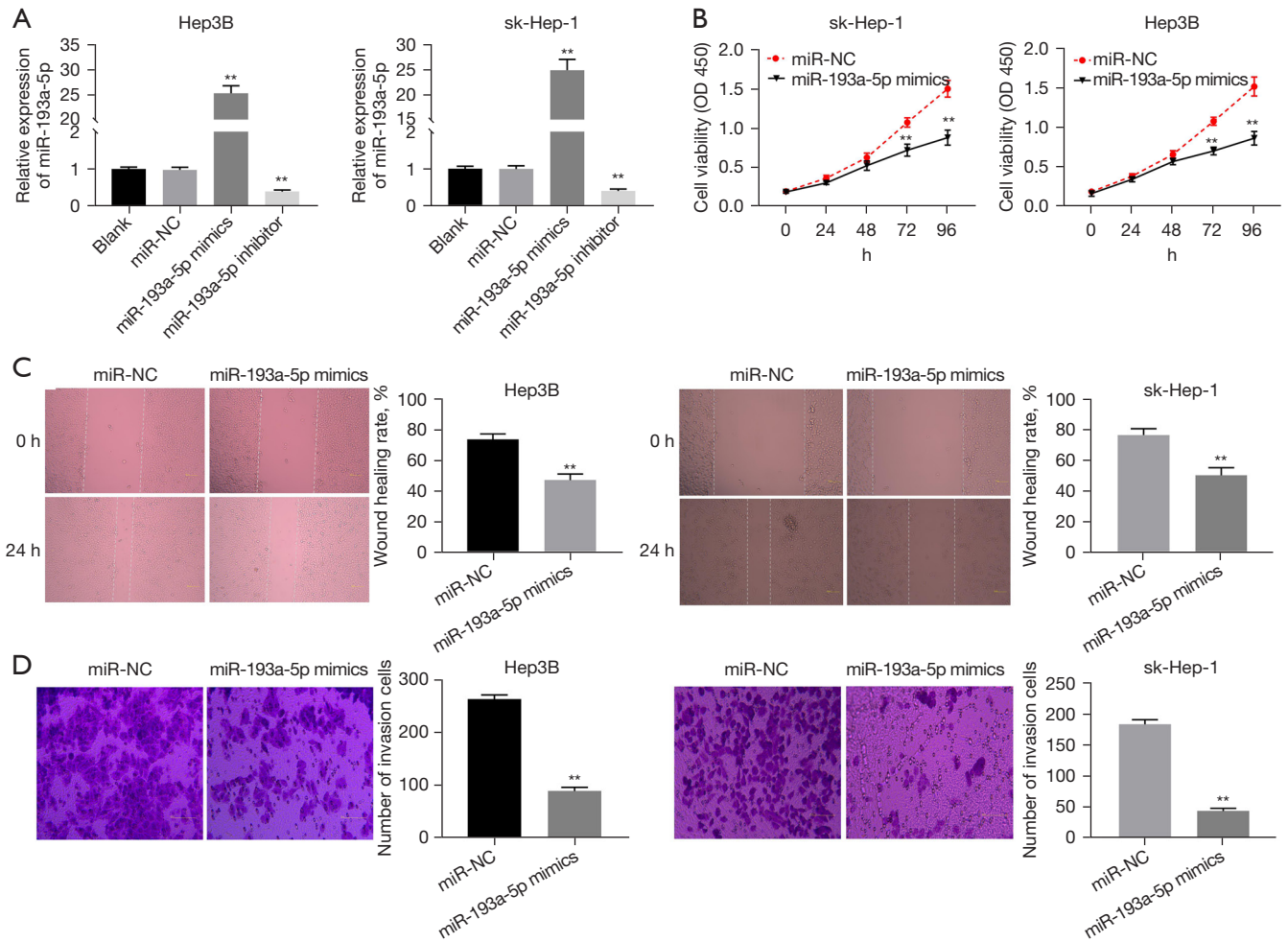

Figure 4 *MiR-193a-5p* overexpression suppressed proliferation, migration, and invasion in HCC cells. (A) *MiR-193a-5p* expression in the transfected Hep3B and sk-Hep-1 cells; (B) cell viability was assessed by MTT assays; (C) migration was measured by wound-healing assays (scar bar =100 μm, ×200); (D) invasion was detected by transwell assays (crystal violet staining, scar bar =100 μm, ×400). **, P<0.01 *vs.* Blank (A) or miR-NC (B-D). miR-193a-5p, microRNA 193a-5p; HCC, hepatocellular carcinoma; MTT, 3-(4,5-dimethylthiazol-2-yl)-2,5-diphenyl-2H-tetrazolium bromide.

wound-healing rate, and number of invasion cells were all significantly more reduced in the miR-193a-5p mimics group than the miR-NC group (P<0.01, *Figure 4B-4D*). Above all, *miR-193a-5p* overexpression restrained cell viability, migration, and invasion in HCC.

MiR-193a-5p directly targeted CDK8

As *Figure 5A* shows, TargetScan predicted the possible target region between *CDK8* and *miR-193a-5p*. The DLR assay results showed that *miR-193a-5p* overexpression clearly decreased the luciferase activity of the cells co-transfected with *CDK8* WT but not that of those co-transfected with *CDK8* Mut (P<0.01). *HEIH* overexpression partially attenuated the reduction action of *miR-193a-5p* mimics on the luciferase activity of *CDK8* WT (P<0.05, *Figure 5B*). In the RIP assays, both the expression of *miR-193a-5p* and *CDK8* were more highly enriched in the AGO2 immunoprecipitate than the IgG immunoprecipitate (P<0.01, *Figure 5C*). Further, *CDK8* expression was significantly more enhanced in the HCC tissues than the adjacent tissues (P<0.001, *Figure 5D*). In terms of the expression level, a negative correlation was observed between *miR-193a-5p* and *CDK8* (r=–0.3419, P=0.008,

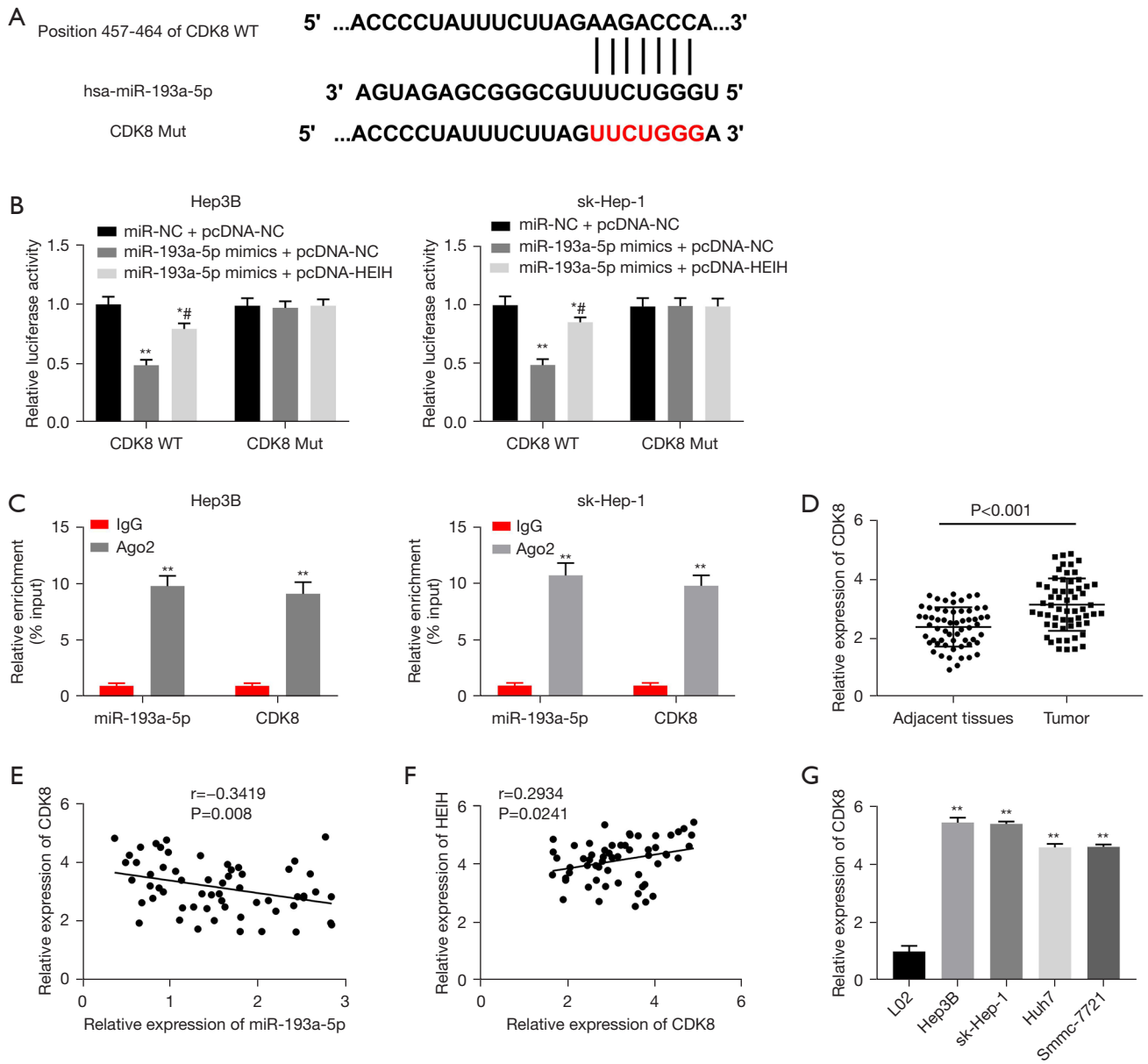

Figure 5 *CDK8* was a direct target of *miR-193a-5p*. (A) The binding sites between *CDK8* and *miR-193a-5p* were predicted by TargetScan; (B) the target correlation between *CDK8* and *miR-193a-5p* was validated by DLR assays; (C) the combination between miR-193a-5p and CDK8 was evaluated by RIP assays; (D) CDK8 expression was detected in the HCC tissues and adjacent tissues; (E,F) a Spearman's correlation analysis was performed to analyze the association between the expression of *CDK8* and *miR-193a-5p* or *HEIH*; (G) *CDK8* expression in the HCC cell lines. *, P<0.05 and **, P<0.01 *vs.* miR-NC + pcDNA-NC (B), IgG (C) or L02 (G); #, P<0.05 *vs.* miR-193a-5p mimics + pcDNA-NC (B). CDK8, cyclin-dependent kinase 8; miR-193a-5p, microRNA 193a-5p; DLR, dual luciferase reporter; RIP, RNA immunoprecipitation; HCC, hepatocellular carcinoma; IgG, immunoglobulin G; HEIH, high expression in hepatocellular carcinoma.

Figure 5E), while a positive correlation was observed between *CDK8* and *HEIH* (r=0.2934, P=0.0241, *Figure 5F*). Additionally, *CDK8* was highly expressed in the Hep3B, sk-Hep-1, Huh7, and Smmc-7721 cells (P<0.01, *Figure 5G*).

Silencing HEIH-1 impeded cell viability, migration, and invasion in HCC via the miR-193a-5p/CDK8 axis

To examine the interactions among *HEIH*, *miR-193a-5p*,

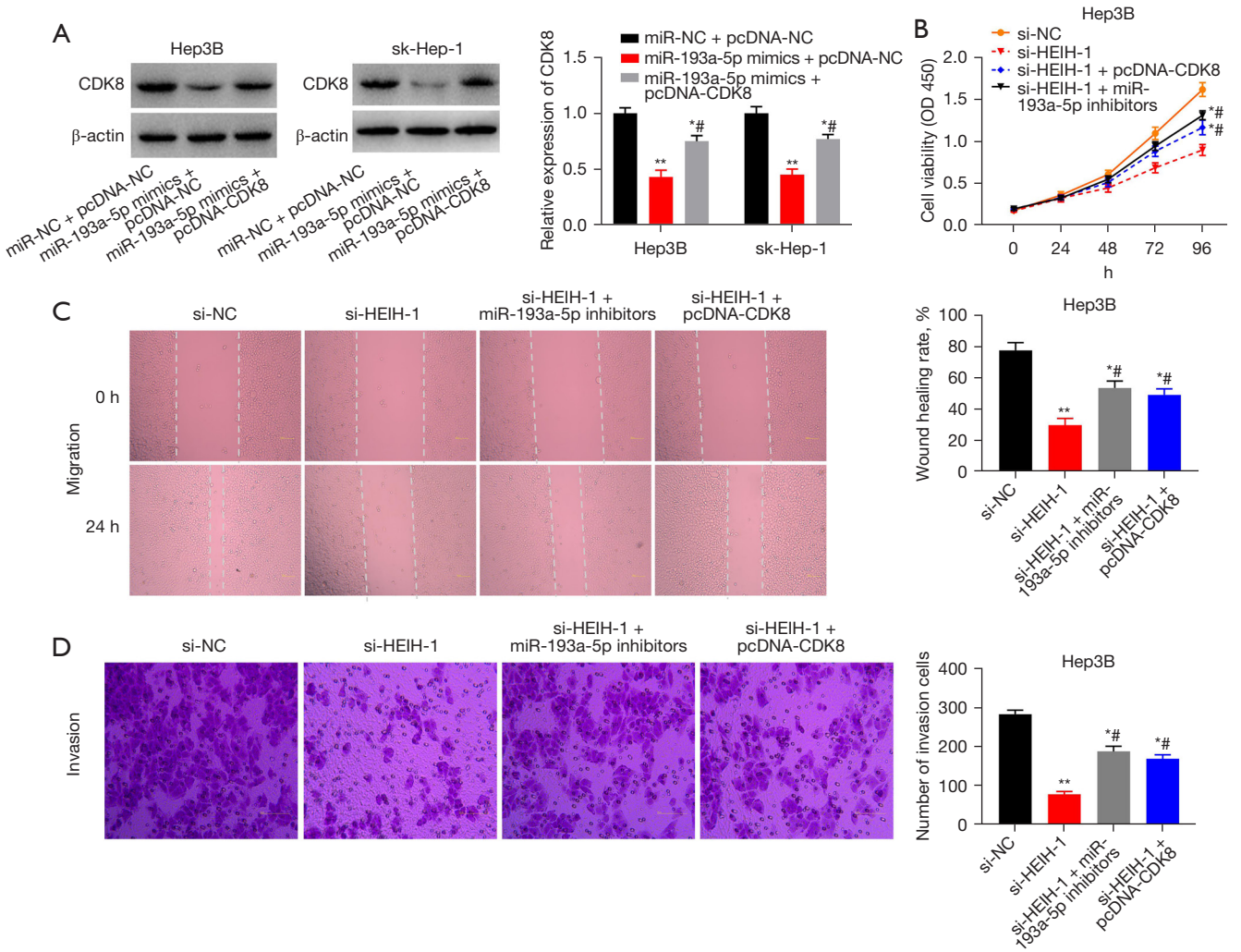

Figure 6 *HEIH* regulated the proliferation, migration and invasion of the HCC cells via *miR-193a-5p/CDK8* axis. (A) Protein expression of CDK8 was detected by Western blot; (B) cell viability was determined by MTT assays; (C,D) migration and invasion were assessed by wound-healing (scar bar =100 μm, ×200) and a transwell assays (crystal violet staining, scar bar =100 μm, ×400). *, P<0.05 and **, P<0.01 *vs.* miR-NC + pcDNA-NC (A) or si-NC (B-D); #, P<0.05 *vs.* miR-193a-5p mimics + pcDNA-NC (A) or si-HEIH-1 (B-D). miR-193a-5p, microRNA 193a-5p; CDK8, cyclin-dependent kinase 8; HEIH, high expression in hepatocellular carcinoma; MTT, 3-(4,5-dimethylthiazol-2-yl)-2,5-diphenyl-2H-tetrazolium bromide; HCC, hepatocellular carcinoma.

and *CDK8* in HCC progression, the Hep3B cells were co-transfected with *miR-193a-5p* mimics/miR-NC and pcDNA-NC/pcDNA-*HEIH*. The Western blot results revealed that the protein expression of CDK8 was significantly decreased by miR-193a-5p overexpression, and the downregulated CDK8 was attenuated by HEIH overexpression (P<0.05, *Figure 6A*). As *Figure 6B* shows, cell viability was decreased by *HEIH* silencing, and the decreased viability was attenuated by *CDK8* overexpression or *miR-193a-5p* downregulation (P<0.05). Both the wound-healing rate and the number of invasion cells were significantly inhibited by *HEIH*-1 silencing, and *miR-193a-5p* inhibition or *CDK8* overexpression partly reversed the decreased wound-healing rate and the number of invasion cells (P<0.05, *Figure 6C,6D*). Thus, silencing *HEIH* impeded cell viability, migration, and invasion in HCC by modulating the *miR-193a-5p/CDK8* axis.

Discussion

The regulatory effects of lncRNA in multiple cancers have

been investigated in recent years (30,31). This research showed that *HEIH* knockdown hampered the viability, migration, and invasion of HCC cells. Additionally, *miR-193a-5p* was a target molecular of *HEIH* and directly targeted *CDK8*. These discoveries will inform further investigations of HCC.

Thousands of lncRNAs have been identified by sequencing human transcriptomes (32). Numerous studies have shown that cancer-related lncRNAs play a crucial role in the initiation and development of HCC (10,33-35). *HEIH* is a newly identified lncRNA and has been explored in multiple cancers, such as cholangiocarcinoma (36), endometrial cancer (37), and breast cancer (38), in recent years. The current investigation showed that *HEIH* was significantly upregulated in HCC tissues and cells. Moreover, the increased expression of *HEIH* was related to an advanced TNM stage and the absence of vascular invasion. These results imply that *HEIH* could be used to predict the poor prognosis of HCC patients. A recent study also illustrate that *HEIH* is highly upregulated in HCC tissues (17). Another report revealed that *HEIH* is significantly overexpressed in HCC tissues and cells, and that silencing *HEIH* inhibits viability, migration, and invasion in HCC (39). The findings of the present study are consistent with these previous studies. Further, this study showed that the knockdown of *HEIH* impeded cell viability, migration, and invasion in HCC. The *in vivo* experiments showed that *HEIH* silencing repressed HCC tumor growth in mice. All these data suggest that *HEIH* exerts an oncogenic effect in HCC tumorigenesis.

There is increasing evidence that lncRNAs can function as competing endogenous RNAs (ceRNAs) to sponge miRNAs, thus affecting the biological function of miRNAs (40). LncRNA *SNHG7* has been shown to accelerate the progression of HCC via the *miR-122-5p*/forkhead box K2 (*FOXK2*) axis (41). Wang *et al.* show that the downregulation of lncRNA *HEIH* suppresses the progression of esophageal squamous cell carcinoma via *miR-4458*/PBX homeobox 3 (*PBX3*) (42). In HCC, the knockdown of *HEIH* suppresses cell viability, migration and invasion via *miR-199a-3p* sponging (17). The present study shows that *HEIH* acts as a ceRNA to sponge *miR-193a-5p*.

Previous studies have explored the effects of *miR-193a-5p* in various cancers. For example, *miR-193a-5p* is downregulated in colorectal cancer, and its downregulation is associated with metastasis and poor prognosis (43). *MiR-193a-5p* is observed to be downregulated in HCC, and the overexpression of *miR-193a-5p* is shown to restrain HCC cell growth and invasion (28). Consistent with previous studies, this study showed that *miR-193a-5p* was downregulated in HCC, and its overexpression impeded the viability, migration, and invasion of HCC cells. Further, *miR-193a-5p* expression was inversely modulated by *HEIH* in HCC. These findings suggest that *HEIH* has a pro-tumor role in HCC progression possibly by negatively regulating *miR-193a-5p* expression.

CDK8 is a transcription factor and has a pro-tumor role in diverse human cancers, and is thus considered a potential drug target for cancer therapy (44). Research has shown that CDK8 and CDK19 are highly expressed in prostate cancer, and their inhibitors can curb the metastasis of prostate cancer (45). In a previous report, a novel CDK8 inhibitor was shown to suppress the metastasis of prostate cancer *in vivo* and *in vitro* (46). Additionally, *LINC01224* is reported to contribute to the malignant process of gastric cancer via the *miR-193a-5p*/*CDK8* axis (47). Yin *et al.* report that *CDK8* is significantly upregulated in HCC, and directly targets *miR-152-3p* (48). Similarly, the present study showed that *CDK8* expression was strongly enhanced in HCC, and *miR-193a-5p* directly targeted *CDK8*. More importantly, it also showed that the inhibitory function of *HEIH* silencing on the viability, migration, and invasion of HCC cells was partially rescued by *miR-193a-5p* inhibition or *CDK8* overexpression, suggesting that *HEIH* exerted a pro-tumor effect in the progression of HCC likely by regulating the *miR-193a-5p*/*CDK8* axis.

Conclusions

In summary, the results showed that *HEIH* was prominently upregulated in HCC, and *HEIH* expression was closely related to TNM stage and vascular invasion. Additionally, silencing *HEIH* inhibited the viability, migration, and invasion of HCC cells *in vitro*, and impeded HCC tumor growth *in vivo*. The anti-tumor effect of silenced *HEIH* might be exerted via the targeting of *miR-193a-5p* and *CDK8*. More research needs to be conducted to explore the effects of *HEIH* on other cells related to HCC; however, the current research provides a helpful perspective on interference of *HEIH* with HCC.

Acknowledgments

Funding: The project was supported by the Hainan Provincial Natural Science Foundation (No. 821MS0833) and the Hainan Province Clinical Medical Center of China.

Footnote

Reporting Checklist: The authors have completed the MDAR and ARRIVE reporting checklists. Available at https://tcr.amegroups.com/article/view/10.21037/tcr-23-2228/rc

Data Sharing Statement: Available at https://tcr.amegroups.com/article/view/10.21037/tcr-23-2228/dss

Peer Review File: Available at https://tcr.amegroups.com/article/view/10.21037/tcr-23-2228/prf

Conflicts of Interest: All authors have completed the ICMJE uniform disclosure form (available at https://tcr.amegroups.com/article/view/10.21037/tcr-23-2228/coif). The authors have no conflicts of interest to declare.

Ethical Statement: The authors are accountable for all aspects of the work in ensuring that questions related to the accuracy or integrity of any part of the work are appropriately investigated and resolved. This study was conducted in accordance with the Declaration of Helsinki (as revised in 2013). The study was approved by the Ethics Committee of The Second Affiliated Hospital of Hainan Medical University (No. LW20210018). Informed consent was taken from all the patients. All animal experiments were approved by the Ethics Committee of the Second Affiliated Hospital of Hainan Medical University (No. LW20210018), in compliance with national guidelines for the care and use of animals.

References

1. Vogel A, Meyer T, Sapisochin G, et al. Hepatocellular carcinoma. Lancet 2022;400:1345-62.
2. Sy AM, Ferreira RD, John BV. Hepatocellular Carcinoma in Primary Biliary Cholangitis. Clin Liver Dis 2022;26:691-704.
3. Yang TH, Chan C, Yang PJ, et al. Genetic Susceptibility to Hepatocellular Carcinoma in Patients with Chronic Hepatitis Virus Infection. Viruses 2023;15:559.
4. Liccioni A, Reig M, Bruix J. Treatment of hepatocellular carcinoma. Dig Dis 2014;32:554-63.
5. Crocetti L, Bargellini I, Cioni R. Loco-regional treatment of HCC: current status. Clin Radiol 2017;72:626-35.
6. Cong WM, Wu MC. New insights into molecular diagnostic pathology of primary liver cancer: Advances and challenges. Cancer Lett 2015;368:14-9.
7. Quinn JJ, Chang HY. Unique features of long non-coding RNA biogenesis and function. Nat Rev Genet 2016;17:47-62.
8. Shao T, Xie Y, Shi J, et al. Surveying lncRNA-lncRNA cooperations reveals dominant effect on tumor immunity cross cancers. Commun Biol 2022;5:1324.
9. Shaath H, Vishnubalaji R, Elango R, et al. Long non-coding RNA and RNA-binding protein interactions in cancer: Experimental and machine learning approaches. Semin Cancer Biol 2022;86:325-45.
10. Farzaneh M, Ghasemian M, Ghaedrahmati F, et al. Functional roles of lncRNA-TUG1 in hepatocellular carcinoma. Life Sci 2022;308:120974.
11. Cai Y, Lyu T, Li H, et al. LncRNA CEBPA-DT promotes liver cancer metastasis through DDR2/β-catenin activation via interacting with hnRNPC. J Exp Clin Cancer Res 2022;41:335.
12. Sun JY, Ni MM. Long non-coding RNA HEIH: a novel tumor activator in multiple cancers. Cancer Cell Int 2021;21:558.
13. Wang X, Chen Z, Zhou H, et al. LncRNA HEIH expression in cancer prognosis: A review and meta-analysis. Medicine (Baltimore) 2023;102:e33970.
14. Zhang H, Shen X, Xiong S, et al. HEIH Promotes Malignant Progression of Gastric Cancer by Regulating STAT3-Mediated Autophagy and Glycolysis. Dis Markers 2022;2022:2634526.
15. He C, Huang D, Yang F, et al. High Expression of lncRNA HEIH is Helpful in the Diagnosis of Non-Small Cell Lung Cancer and Predicts Poor Prognosis. Cancer Manag Res 2022;14:503-14.
16. Zhao J, Meng R, Yao Q, et al. Long non-coding RNA HEIH promotes breast cancer development via negative modulation of microRNA-200b. Pharmazie 2019;74:471-6.
17. Ma Y, Cao D, Li G, et al. Silence of lncRNA HEIH suppressed liver cancer cell growth and metastasis through miR-199a-3p/mTOR axis. J Cell Biochem

2019;120:17757-66.
18. Shukla GC, Singh J, Barik S. MicroRNAs: Processing, Maturation, Target Recognition and Regulatory Functions. Mol Cell Pharmacol 2011;3:83-92.
19. He L, Hannon GJ. MicroRNAs: small RNAs with a big role in gene regulation. Nat Rev Genet 2004;5:522-31.
20. Hayes J, Peruzzi PP, Lawler S. MicroRNAs in cancer: biomarkers, functions and therapy. Trends Mol Med 2014;20:460-9.
21. Huang YH, Lian WS, Wang FS, et al. MiR-29a Curbs Hepatocellular Carcinoma Incidence via Targeting of HIF-1α and ANGPT2. Int J Mol Sci 2022;23:1636.
22. Yang Y, Yang T, Zhao Z, et al. Down-regulation of BMAL1 by MiR-494-3p Promotes Hepatocellular Carcinoma Growth and Metastasis by Increasing GPAM-mediated Lipid Biosynthesis. Int J Biol Sci 2022;18:6129-44.
23. Hong J, Liu J, Zhang Y, et al. MiR-3180 inhibits hepatocellular carcinoma growth and metastasis by targeting lipid synthesis and uptake. Cancer Cell Int 2023;23:66.
24. Wang Y, Li N, Zhao J, et al. MiR-193a-5p serves as an inhibitor in ovarian cancer cells through RAB11A. Reprod Toxicol 2022;110:105-12.
25. Liu Q, Zhao E, Geng B, et al. Tumor-associated macrophage-derived exosomes transmitting miR-193a-5p promote the progression of renal cell carcinoma via TIMP2-dependent vasculogenic mimicry. Cell Death Dis 2022;13:382.
26. Li M, Wu P, Yang Z, et al. miR-193a-5p promotes pancreatic cancer cell metastasis through SRSF6-mediated alternative splicing of OGDHL and ECM1. Am J Cancer Res 2020;10:38-59.
27. Zhang X, Zhang D, Bu X, et al. Identification of a novel miRNA-based recurrence and prognosis prediction biomarker for hepatocellular carcinoma. BMC Bioinformatics 2022;23:479.
28. Li P, Xiao Z, Luo J, et al. MiR-139-5p, miR-940 and miR-193a-5p inhibit the growth of hepatocellular carcinoma by targeting SPOCK1. J Cell Mol Med 2019;23:2475-88.
29. Wang JT, Wang ZH. Role of miR-193a-5p in the proliferation and apoptosis of hepatocellular carcinoma. Eur Rev Med Pharmacol Sci 2018;22:7233-9.
30. Li Y, Jiang T, Zhou W, et al. Pan-cancer characterization of immune-related lncRNAs identifies potential oncogenic biomarkers. Nat Commun 2020;11:1000.
31. Park EG, Pyo SJ, Cui Y, et al. Tumor immune microenvironment lncRNAs. Brief Bioinform 2022;23:bbab504.
32. Liao HT, Huang JW, Lan T, et al. Identification of The Aberrantly Expressed LncRNAs in Hepatocellular Carcinoma: A Bioinformatics Analysis Based on RNA-sequencing. Sci Rep 2018;8:5395.
33. Huang Z, Zhou JK, Peng Y, et al. The role of long noncoding RNAs in hepatocellular carcinoma. Mol Cancer 2020;19:77.
34. Xu K, Xia P, Gongye X, et al. A novel lncRNA RP11-386G11.10 reprograms lipid metabolism to promote hepatocellular carcinoma progression. Mol Metab 2022;63:101540.
35. Li Y, Hu J, Guo D, et al. LncRNA SNHG5 promotes the proliferation and cancer stem cell-like properties of HCC by regulating UPF1 and Wnt-signaling pathway. Cancer Gene Ther 2022;29:1373-83.
36. Wan T, Wang H, Gou M, et al. LncRNA HEIH promotes cell proliferation, migration and invasion in cholangiocarcinoma by modulating miR-98-5p/HECTD4. Biomed Pharmacother 2020;125:109916.
37. Guo JL, Tang T, Li JH, et al. LncRNA HEIH Enhances Paclitaxel-Tolerance of Endometrial Cancer Cells via Activation of MAPK Signaling Pathway. Pathol Oncol Res 2020;26:1757-66.
38. Nafea H, Youness RA, Abou-Aisha K, et al. LncRNA HEIH/miR-939-5p interplay modulates triple-negative breast cancer progression through NOS2-induced nitric oxide production. J Cell Physiol 2021;236:5362-72.
39. Shen Q, Jiang S, Wu M, et al. LncRNA HEIH Confers Cell Sorafenib Resistance in Hepatocellular Carcinoma by Regulating miR-98-5p/PI3K/AKT Pathway. Cancer Manag Res 2020;12:6585-95.
40. Chan JJ, Tay Y. Noncoding RNA:RNA Regulatory Networks in Cancer. Int J Mol Sci 2018;19:1310.
41. Zhao Z, Gao J, Huang S. LncRNA SNHG7 Promotes the HCC Progression Through miR-122-5p/FOXK2 Axis. Dig Dis Sci 2022;67:925-35.
42. Wang D, You D, Pan Y, et al. Downregulation of lncRNA-HEIH curbs esophageal squamous cell carcinoma progression by modulating miR-4458/PBX3. Thorac Cancer 2020;11:1963-71.
43. Zhang P, Ji DB, Han HB, et al. Downregulation of miR-193a-5p correlates with lymph node metastasis and poor prognosis in colorectal cancer. World J Gastroenterol 2014;20:12241-8.
44. Wu D, Zhang Z, Chen X, et al. Angel or Devil ? - CDK8 as the new drug target. Eur J Med Chem 2021;213:113043.

45. Offermann A, Joerg V, Becker F, et al. Inhibition of Cyclin-Dependent Kinase 8/Cyclin-Dependent Kinase 19 Suppresses Its Pro-Oncogenic Effects in Prostate Cancer. Am J Pathol 2022;192:813-23.
46. Ho TY, Sung TY, Pan SL, et al. The study of a novel CDK8 inhibitor E966-0530-45418 that inhibits prostate cancer metastasis in vitro and in vivo. Biomed Pharmacother 2023;162:114667.
47. Sun H, Yan J, Tian G, et al. LINC01224 accelerates malignant transformation via MiR-193a-5p/CDK8 axis in gastric cancer. Cancer Med 2021;10:1377-93.
48. Yin T, Liu MM, Jin RT, et al. miR-152-3p Modulates hepatic carcinogenesis by targeting cyclin-dependent kinase 8. Pathol Res Pract 2019;215:152406.

Cite this article as: Huang Y, Li D, Lu L, Song D, Li P. LncRNA *HEIH* modulates the proliferation, migration, and invasion of hepatocellular carcinoma cells by regulating the *miR-193a-5p/CDK8* axis. Transl Cancer Res 2024;13(1):423-436. doi: 10.21037/tcr-23-2228

